

Prediction of Sulfur in the Hot Metal based on Data Mining and Artificial Neural Networks

Wandercleiton Cardoso^a and Rendo di Felice^b

*Dipartimento di Ingegneria Civile, Chimica e Ambientale (DICCA), Università degli Studi di Genova,
Via All'Opera Pia, 15, CAP 16145, Genova (GE), Italy*

Keywords: Big Data, Machine Learning, Blast Furnace, Sulfur, Industry 4.0.

Abstract: In recent years, interest in artificial intelligence and the integration of Industry 4.0 technologies to improve and monitor steel production conditions has increased. In the current scenario of the world economy, where the prices of energy and inputs used in industrial processes are increasingly volatile, strict control of all stages of the production process is of paramount importance. For the steel production process, the temperature of the metal in the liquid state is one of the most important parameters to be evaluated, since its lack of control negatively affects the final quality of the product. Every day, several models are proposed to simulate industrial processes. In this sense, data mining and the use of artificial neural networks are competitive alternatives to solve this task. In this context, the objective of this work was to perform data mining in a Big Data with more than 300,000 pieces of information, processing them using an artificial neural network and probabilistic reasoning. It is concluded that data mining and neural networks can be used in practice as a tool for predicting and controlling impurities during the production of hot metal in a blast furnace.

1 INTRODUCTION

The blast furnace is a chemical-metallurgical reactor used to produce molten iron, which is the product formed by the reduction of metallic oxides that chemically react with reducing elements such as carbon monoxide (CO) and hydrogen gas (H₂) (Chizhikova and Best, 2020).

Blast furnaces are chemical metallurgical reactors for the production of pig iron and slag. Pig iron is obtained in a liquid state and consists of iron (92 to 95%), carbon (3 to 4.5%) and impurities such as sulphur, phosphorus and silica (Arif and Ahmad, 2021).

The raw materials used (metallic feedstock) are sinter, granulated ore and pellets. The main fuel is metallurgical coke. All these materials are loaded through the upper part of the reactor, with hot air blown into the lower section (Zhao et al., 2020).


The injected hot air gasifies the coke and produces CO reducing gas and a large amount of heat that rises upwards in counter current to the descent of the charge, providing heating, reduction and melting


of the metallic charge. Pulverized coal is used as an additional fuel, which is blown in together with hot air (Blotevogel, 2021).

The preheated air with a temperature of about 1200°C is blown through the blast tuyeres of the blast furnace and comes into contact with the coke in the raceway area. The contact of the oxygen in the air with the carbon of the coke heated to 1500°C first leads to a reaction that produces carbon dioxide (CO₂) (Zhang et al., 2019a).

This highly exothermic reaction generates a large amount of heat for the process. The carbon dioxide immediately reacts with the carbon in the coke to form carbon monoxide (CO), according to the loss-of-solution or Boudouard reaction ($C + CO_2 \rightarrow 2CO$), which is very endothermic (Cardoso et al., 2021b).

The moisture contained in the injected air reacts with the carbon in the coke to produce the reducing gases CO and H₂. Although these reactions are endothermic, i.e. proceed under heat absorption, the exit of the reducing gases from the duct effectively results in a high heat input into the process, producing

^a  <https://orcid.org/0000-0001-8531-4049>

^b  <https://orcid.org/0000-0002-8169-3325>

flame temperatures in excess of 2000°C (Fontes et al., 2020; Cardoso et al., 2021a; Cardoso et al., 2022).

On the rest of the way through the furnace, the rising gas gives off heat to the descending metal layers and leaves the furnace with temperatures in the order of 100 to 150°C (Kurunov, 2019).

Due to the different heat requirements for a number of chemical reactions taking place at different levels in the furnace, the temperature profile takes on a characteristic shape: an upper preheating zone (0-800°C) separated from a lower melting zone (900-1500°C) and a vertical thermal reserve zone whose temperature is in the range of 800-1000°C (Ibragimov et al., 2019; Kong et al., 2021).

The thermal reserve zone, where there is little heat exchange between gas and solids, occupies 40-50% of the total height of the furnace (Kurunov, 2018).

The nature of the countercurrent process allows a highly reducing gas (high content of CO) to contact the metallic mineral wustite, which has the lowest oxygen potential of the iron oxides, and then hematite and magnetite in the upper zone to be reduced by a gas with a lower reduction potential (Li et al., 2021a).

Since CO₂ is the end product of carbon combustion, the more oxygen that is removed, the more complete the utilisation of the thermal and chemical energy of the carbon (Li et al., 2021b).

These reactions are called indirect reduction, and the overall reaction is slightly exothermic. If some of the wustite remains unreduced, it is further reduced by direct reduction in the range where temperatures exceed 1000°C (Matino et al., 2019a).

The high temperature ramp gas generated in the combustion zone (the tuyeres region) causes heating of the charge, decomposition reactions and reduction of oxides during its ascent in the blast furnace. As a result, the temperature of the gas gradually decreases while its chemical composition changes (Muraveva et al., 2021; Pavlov et al., 2019).

First, near the charge level, the charge undergoes moisture evaporation and preheating. When the charge descends, the reduction of iron oxides takes place. In the softening and melting zone, in the area of the lower vat and the belly, begins the softening and melting of the charge, which develops to the crucible (Cardoso et al., 2022).

The pig iron (hot metal) and slag that are in the crucible are removed at controlled intervals through the running holes. In the area of the tuyeres, the coke gradually decreases in size as it burns (Rasul et al., 2007; Saxén and Pettersson, 2007).

Together with the fusion of the materials that make up the charge, this causes the level in the blast

furnace to drop, so that a new charge has to be conveyed at the top (Semenov et al., 2020).

Coke is considered the permeabilizer of the blast furnace charge. This role cannot be assumed by any other fuel, as coke is the only material capable of maintaining the permeability of the bed to the ascending gas, as well as that of the descending liquid slag and hot metal (Tan et al., 2020).

Coke remains solid under the high-temperature conditions prevailing in the oven and maintains levels of resistance to the different stresses it undergoes inside the oven. This allows it to maintain a suitable size and size distribution for good permeability, without which the manufacture of pig iron in a blast furnace would be impossible (Cardoso et al., 2022).

However, the thermal and chemical roles can be played, in part, by other liquid fuels (petroleum fuel oil and coal tar), gaseous with high calorific value (reducing gas, natural gas, and coke oven gas) or solids (mainly, mineral coal), injected through the tuyeres of the kiln. Thus, these auxiliary fuels also participate as sources of heat and reducing gas for the process. Figure 1 illustrates the working principle of a blast furnace:

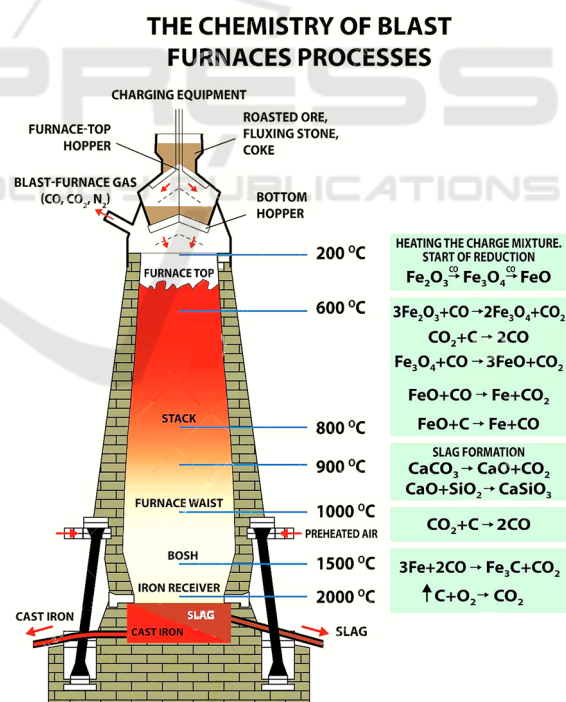


Figure 1: Blast furnace working principle.

Blast furnace monitoring is of paramount importance in the production of a quality product. Sulfur in steel is an undesirable residue that

negatively affects properties such as ductility, toughness, weldability and corrosion resistance.

In recent years, the demand for steels with higher toughness and ductility has increased, and low sulfur levels are important to achieve these properties. Furthermore, sulfur may play an important role in some corrosion processes in steel.

Therefore, in the production of steel for the pipe and automotive industries, for example, the control of the sulfur content is fundamental. The production of low sulfur steel is of utmost importance for shipbuilding and pipelines for the oil industry. This requires high production control in the blast furnace and an efficient desulfurization process at the lowest possible cost.

In the field of technology and modelling, in addition to predicting the effects of changes in production parameters, several blast furnace simulation models have been developed with the aim of improving production conditions, including two- and three-dimensional models that allow progress and detailed information on fluid flow and mass and heat balances within the blast furnace.

Considering the existing difficulties in the field of simulation of complex processes, the application of solutions based on neural networks has gained space due to its diversity of application and increase in the reliability of responses, since the neural network receives new data in the operating process/training without necessarily drawing conclusions about values or types of interaction between raw materials for the use of neural models.

In computer science and related fields, artificial neural networks are computational models inspired by an animal's central nervous system (in particular the brain) that are capable of performing machine learning as well as pattern recognition. Artificial neural networks are generally presented as systems of "interconnected neurons, which can compute input values", simulating the behaviour of biological neural networks. Figure 2 illustrates an artificial neural network.

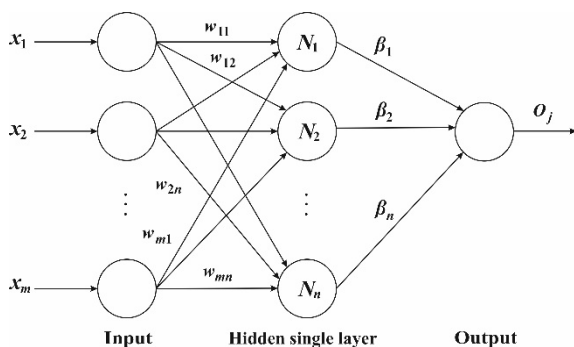


Figure 2: Artificial neural network.

The objective of this work is to mine a database and numerically simulate an artificial neural network with 25 neurons in the hidden layer.

2 RESEARCH METHOD

The database used for numerical simulation corresponds to 11 years of reactor operation. Big Data contains 301,125 pieces of information divided into 75 variables. The neural network input is composed of 74 input variables and 1 output variable.

The artificial neural network has a structure similar to Figure 3 with a simple layer and 25 neurons in the hidden layer, using the Levenberg-Marquardt training algorithm, and a sigmoid activation function.

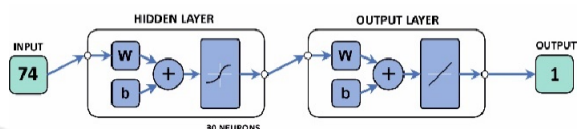


Figure 3: Artificial neural network architecture.

According to the literature, 85% of the database should be used to train and validate the neural network and the remaining 15% will be used to test the model's predictive capacity during the test step. Table 1 illustrates the database division. Table 2 to 8 illustrates the input variable and Table 9 illustrates the output variable

Table 1: Division of samples.

Step	Samples
Training	210.789
Validation	45.168
Test	45.168

Table 2: Blast Furnace Gas.

Variable	Mean	Std_dev
CO (%)	23.8	0.74
CO ₂ (%)	24.3	0.66
N ₂ (%)	47.2	1.39
H ₂ (%)	4.50	0.43
CO + CO ₂	47.9	0.6
CO efficiency (%)	49.5	0.85
H ₂ efficiency (%)	40.7	3.25

Table 3: Hot metal.

Variable	Mean	Std_dev
Estim. Production (ton)	7789.5	314.5
Real production (ton)	7787.2	324.5
Carbon (%)	4.635	0.169
Chrome (%)	0.025	0.002
Copper (%)	0.007	0.001
Manganese (%)	0.29	0.03
Mn ratio (-)	0.13	0.22

Table 4: Slag.

Variable	Mean	Std_dev
Slag rate (kg/ton)	246.99	13.74
B2 basicity (-)	1.2	0.04
B4 basicity (-)	1.07	0.04
Al ₂ O ₃ (%)	10.71	0.62
CaO (%)	43.06	1.55
Sulfur (%)	1.15	0.14
FeO (%)	0.42	0.04
MgO (%)	6.83	0.86
MnO (%)	0.31	0.1
SiO ₂ (%)	36.05	1.36
TiO ₂ (%)	0.58	0.05
Production (ton)	1980.6	190.8
Mn ratio (-)	0.87	0.22

Table 5: Fuel.

Variable	Mean	Std_dev
Injection PCI (kg/ton)	58.99	6.16
Gas rate (kg/ton)	-	-
Coal/O ₂ tax (-)	755.27	75.57
Coal/air tax (-)	170.03	74.12
PCI rate	175.98	15.61
Direct reduction (%)	23.38	12.41
PCI tax (kg/ton)	1078.3	540.9
Coke total (kg/ton)	1932.2	911.7
Small coke (kg/ton)	294.63	134.86
Coke 1 (kg/ton)	210.7	259.8
Coke 2 (kg/ton)	742	716
Coke 3 (kg/ton)	946	956
Coke 4 (kg/ton)	1878	143
Coke 5 (kg/ton)	1327.5	847.6
Moisture (kg/ton)	6.4	1.41
Coke/load (kg/ton)	11.89	9.56
Small coke total (kg/ton)	4.28	0.03
PCI/load (kg/ton)	174.74	14.32
Fuel rate/load (kg/ton)	484.08	18.14
Coke total/load (kg/ton)	24.52	0.89
PCI/day (-)	1214.4	44.9
Coke rate (kg/ton)	319.68	25.98

Table 6: Thermal control.

Variable	Mean	Std_dev
Hot metal (°C)	1508.3	12.2
Blowing air (°C)	1243.3	13.9
Top gas (°C)	121,35	10,34
Flame temperature (°C)	2177.6	2108
Slag	1508.3	12.2
Thermal index (-)	504.7	54.03

Table 7: Minerals.

Variable	Mean	Std_dev
Ore/Coque (-)	5.1	0.31
Sinter 1 (ton)	4536.3	884.2
Sinter 2 (ton)	1697.2	1326.2
Pellet 1 (ton)	5132	1898.3
Pellet 2 (ton)	4813.7	2183.1
Total metal load (ton)	12312	670
Raw material rate	1578.8	15.1
Ore (%)	8.9	4.5
Sinter (%)	39.6	2.8
Pellet (%)	51.5	5.1
Ore (day)	12747	703

Table 8: Blow air.

Variable	Mean	Std_dev
Volume (Nm ³ /min)	4852.9	148.6
Pressure (Kgf/cm ²)	3.87	0.1
Moisture (kg/m ³)	19.81	3.73
O ₂ enrichment (%)	5.27	0.95
Steam (%)	1.51	1.01
Consumption (Nm ³ /min)	7030.3	213.6

Table 9: Sulfur output (%).

Mean	0.023
Standard deviation	0.008
Minimum	0.008
Median	0.021
Maximum	0.083
Skewness	1.5
Kurtosis	4.8

The method used to evaluate the quality of the neural network model was the RMSE (root mean square error). Small values close to zero indicate better predictive capacity of the model. Pearson's mathematical correlation coefficient (R) was also used to validate the mathematical models.

$$RMSE = \sqrt{\frac{1}{n} \sum_{i=1}^n (C_{neural} - C_{real})^2} \quad (1)$$

$$R = \sqrt{\frac{\sum_{i=1}^n (C_{neural} - C_{real})^2}{\sum_{i=1}^n (C_{real} - C_{neural})^2}} \tag{2}$$

The RMSE mathematical equation is presented in Eq(1) and Pearson's mathematical correlation coefficient is presented in Eq(2).

3 RESULTS AND DISCUSSION

The sulfur prediction model presented greater difficulty in the prediction, but even so, the result was excellent compared to the literature. There was no evidence of overfitting or underfitting in the hot metal sulfur prediction model.

There was no discrepancy between the RMSE values for the training, validation and testing phases. The artificial neural network required a maximum of 687 epochs to converge the model, indicating greater complexity to stabilize the error values.

The mathematical correlation (R) and the RMSE of the artificial neural network is shown in Table 10 e Table 11 and confirms an excellent correlation value. Figure 4 illustrates the dispersion between the values calculated by the neural network and the values of Big Data.

Table 10: Root Mean Square Error.

Overall	0.0027
Training	0.0031
Validation	0.0030
Testing	0.0031

Table 11: Pearson's correlation coefficient.

Overall	0.9632
Training	0.9682
Validation	0.9660
Testing	0.9373

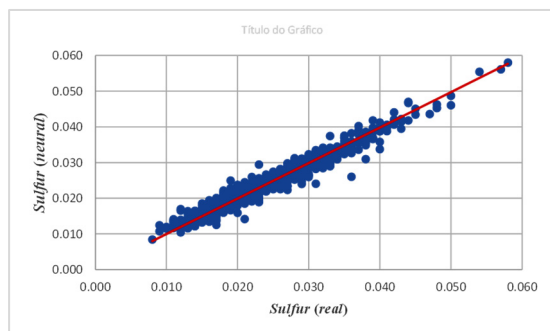


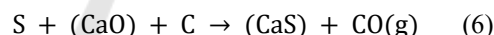
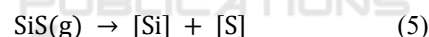
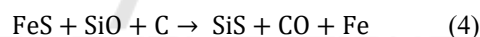
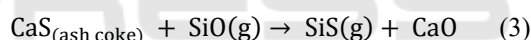
Figure 4: Scatterplot sulfur.

From a metallurgical point of view Most of the sulfur contained in hot metal (about 80%) is introduced into the blast furnace by the metallurgical coke in the form of iron sulfide (FeS) and calcium sulfide (CaS) contained in the coke ash, and as organic sulfur. The rest comes via the other materials in the metallic charge and the fluxes.

In blast furnaces fed with metallurgical coke, about 90 to 80% of the sulfur is part of the chemical composition of the slag, while 10% to 15% is precipitated with the blast furnace gas and values between 2% and 5% dissolve in the hot metal. Recent studies have shown that the main mechanism of sulfur reactions is very similar to that of silicon.

Small amounts of sulfur are also absorbed by the slag in the area of the blast furnace channel. It should also be mentioned that sulfur forms other compounds such as sulfur dioxide (SO₂) and carbon disulfide (CS), which are also transported by the gas stream and undergo chemical reactions. However, it must be emphasized that among sulfur gasses, silicon sulfide (SiS) is the dominant species.

In the blast furnace raceway, the sulfur produced reacts with calcium (Ca), silicon (Si), and iron (Fe) according to Eq.3, Eq. 4, and Eq. 5. The chemical reaction that removes sulfur from the hot metal is often represented by Eq. 6.



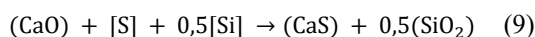
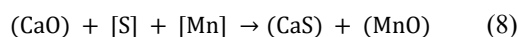
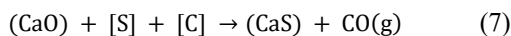
The transfer of sulfur from the gasses to the hot metal takes place in an area of the blast furnace known as the dripping zone. Inside the blast furnace, in the softening and melting zone, when silicon and sulfur-containing hot metal droplets percolate through the slag, in the absence of MnO, the silicon content of the hot metal increases and no transfer of sulfur occurs.

However, in the presence of MnO, silicon is removed from the hot metal and the transfer of manganese from the slag to the metal occurs together with the transfer of sulfur from the metal to the slag. Literature states that gasses such as SiO and SiS are formed in the beneficiation zone, while silicon and sulfur are transferred to the hot metal in the combustion zone.

Silicon is reduced by FeO and MnO and dissolved in the slag while the hot metal droplets penetrate the slag layer. It should be mentioned that CaO has a much greater desulfurization potential than MgO,

about 100 times stronger. It should also be noted that for proper desulfurization, the oxygen content of the metal must be very low.

This is possible due to the reaction of oxygen dissolved in the hot metal with strong oxide forming elements. Thus, if considering the oxide-forming elements, may write the following reactions given in Eq. 7, Eq. 8, and Eq. 9.



The increase of the basicity of the slag increases the CaO activity and favors desulfurization. Low FeO concentrations in the slag favor the incorporation of sulfur into the hot metal. Carbon and silicon dissolved in the hot metal favor desulfurization by increasing the thermodynamic activity of sulfur in the slag.

Considering all this information and the fact that sulfur is an extremely harmful chemical element for steel, the use of a ANN to predict sulfur in metal production is justified.

4 CONCLUSIONS

Regarding simulation methods for predicting process variables, the increasing development of computational capacity, leading to cheaper and more powerful equipment, is driving the development of more complex algorithms with better results, such as neural networks.

Thus, the progress in computational capacity enabled the development of different types of simulation models.

This is one of the factors that enabled the use of the ANN model in this study, as well as the identification of the main variables that affect the model.

The processing of the data to be used for the development of the model is highlighted as an important part of the process, which is sometimes a slow process since the information must be evaluated to find the best way to identify outliers for the development of models.

However, it is important to emphasize that the model in isolation may predict good results for each of the target variables. It should be noted that the use of the above modelling technique has enabled the construction of higher fidelity models that may be used as tools for decision making and operational planning related to fuel economy, operational

stability, and delivery of a product for steelmaking and help improve process monitoring.

In short, neural networks may be used in practice because the model is both a predictive tool and a guide for operation due to the excellent correlations between the real values and the values computed by the neural network.

REFERENCES

- Arif, M. S.; Ahmad, I. Artificial Intelligence Based Prediction of Exergetic Efficiency of a Blast Furnace. *Computer Aided Chemical Engineering*, v.50, pp. 1047-1052, 2021.
- Bai, Y.; Tan, M. Dynamic committee machine with fuzzy-C-means clustering for total organic carbon content prediction from wireline logs. *Computers & Geosciences*, v.146, pp. 104626, 2021.
- Blotevogel, S. Glass structure of industrial ground granulated blast furnace slags (GGBS) investigated by time-resolved Raman and NMR spectroscopies. *Journal of Materials Science*, v.56, pp. 17490-17504, 2021
- Cardoso, W.; Baptista, R.; di Felice, R. Artificial Neural Networks for Modelling and Controlling the Variables of a Blast Furnace. In *IEEE 6th International Forum on Research and Technology for Society and Industry (RTSI)*, pp. 148-152, 2021b.
- Cardoso, W.; Baptista, R.; di Felice, R. Artificial neural network for predicting silicon content in the hot metal produced in a blast furnace fueled by metallurgical coke. *Materials Research*, v.25, pp. 20210439, 2022.
- Cardoso, W.; Baptista, R.; di Felice, R. Mathematical modeling of a solid oxide fuel cell operating on biogas. *Bulletin of Electrical Engineering and Informatics*, v.10, n.06, pp. 2929-2942, 2021c.
- Cardoso, W.; Barros, D.; Baptista, R.; di Felice, R. Mathematical Modelling to Control the Chemical Composition of Blast Furnace Slag Using Artificial Neural Networks and Empirical Correlation. *IOP Conference Series: Materials Science and Engineering*, v.1203, pp. 032096, 2021a.
- Cardoso, W.; di Felice, R. Prediction of silicon content in the hot metal using Bayesian networks and probabilistic reasoning. *International Journal of Advances in Intelligent Informatics*, v.07, n.03, pp. 268-281, 2021d.
- Carro, K. B.; Leite, G. R.; Oliveira, A. G.; Santos, C. B.; Pinto, I. S.; Fux, B.; Falqueto, A. Assessing geographic and climatic variables to predict the potential distribution of the visceral leishmaniasis vector *Lutzomyia longipalpis* in the state of Espírito Santo, Brazil. *Plos One*, v.15, n.9, e0238198, 2020.
- Chen, M.; Wan, X.; Shi, J.; Taskinen, P.; Jokilaakso, A. Experimental Study on the Phase Relations of the SiO₂-MgO-TiO₂ System in Air at 1500°C. *JOM*, v.74, pp. 676-688, 2022
- Chizhikova, V. M. Best Available Techniques in the Blast-Furnace Production. *Metallurgist*, v.64, pp. 13-35, 2020.

- Ducic, N.; Jovicic, A.; Manasijevic, S.; Radisa, R.; Cojbasic, Z.; Savković, B. Application of Machine Learning in the Control of Metal Melting Production Process. *Applied Sciences*, v.10, n.17, pp. 6048-6063, 2020.
- Fontes, D. O. L.; Vasconcelos, L. G.; Brito, R. P. Blast furnace hot metal temperature and silicon content prediction using soft sensor based on fuzzy C-means and exogenous nonlinear autoregressive models. *Computers & Chemical Engineering*, 141, 107028, 2020.
- He, F.; Zhang, L. Prediction model of end-point phosphorus content in BOF steelmaking process based on PCA and BP neural network. *Journal of Process Control*, v.66, pp. 51-58, 2018.
- Hou, Y.; Wu, Y.; Liu, Z.; Han, H.; Wang, P. Dynamic multi-objective differential evolution algorithm based on the information of evolution progress. *Science China Technological Sciences*, v.64, n.08, pp. 1676-1689, 2021.
- Ibragimov, A. F.; Iskhakov, I. I.; Skopov, G. B.; Kirichenko, A. N. Using Oxygen-Enriched Blast During the Operation of Shaft Furnaces of the Mednogorsk Copper-Sulfur Combine LLC. *Metallurgist*, v.63, pp. 62-69, 2019.
- Jantre, S. R.; Bhattacharya, S.; Maiti, T. Quantile Regression Neural Networks: A Bayesian Approach. *Journal of Statistical Theory and Practice*, v.15, n.03, pp. 01-31, 2021.
- Jiang, Y.; Zhou, P.; Yu, G. Multivariate molten iron quality based on improved incremental random vector functional-link networks. *IFAC PapersOnLine*, pp. 290-294, 2018.
- Kang, Y. B. Progress of Thermodynamic Modeling for Sulfide Dissolution in Molten Oxide Slags: Sulfide Capacity and Phase Diagram. *Metallurgical and Materials Transactions B*, v.52, n.05, pp. 2859-2882, 2021.
- Kina, C.; Turk, K.; Atalay, E.; Donmez, I.; Tanyildizi, H. Comparison of extreme learning machine and deep learning model in the estimation of the fresh properties of hybrid fiber-reinforced SCC. *Neural Computing and Applications*, v.33, n.18, pp. 11641-11659, 2021.
- Kong, W.; Liu, J.; Yu, Y.; Hou, X.; He, Z. Effect of $w(\text{MgO})/w(\text{Al}_2\text{O}_3)$ ratio and basicity on microstructure and metallurgical properties of blast furnace slag. *Journal of Iron and Steel Research International*, v.28, n.10, pp. 1223-1232, 2021.
- Kurunov, I. F. Ways of Improving Blast Furnace Smelting Efficiency with Injection of Coal-Dust Fuel and Natural Gas. *Metallurgist*, v.61, n.09, pp. 736-744, 2018.
- Li, J.; Hua, C.; Qian, J.; Guan, X. Low-rank based Multi-Input Multi-Output Takagi-Sugeno fuzzy modeling for prediction of molten iron quality in blast furnace. *Fuzzy Sets and Systems*, v. 421, pp. 178-192, 2021.
- Li, W.; Zhuo, Y.; Bao, J.; Shen, Y. A data-based soft-sensor approach to estimating raceway depth in ironmaking blast furnace. *Powder Technology*, v.390, pp. 529-538, 2021.
- Li, Y.; Zhang, J.; Zhang, S.; Xiao, W. Dual ensemble online modeling for dynamic estimation of hot metal silicon content in blast furnace system. *ISA Transactions*, 2022, article in press.
- Liang, W.; Wang, G.; Ning, X.; Zhang, J.; Li, Y.; Jiang, C.; Zhang, N. Application of BP neural network to the prediction of coal ash melting characteristic temperature. *Fuel*, v.260, 116324, 2020.
- Liu, Y.; Wang, Y.; Chen, L.; Zhao, J.; Wang, W.; Liu, Q. Incremental Bayesian broad learning system and its industrial application. *Artificial Intelligence Review*, v.54, n.05, 2021.
- Matino, I.; Dettori, S.; Colla, V.; Weber, V.; Salame, S. Two innovative modelling approaches in order to forecast consumption of blast furnace gas by hot blast stoves. *Energy Procedia*, v.158, pp. 4043-4048, 2019a.
- Matino, I.; Dettori, S.; Colla, V.; Weber, V.; Salame, S. Application of Echo State Neural Networks to forecast blast furnace gas production: pave the way to off-gas optimized management, *Energy Procedia*, v.158, pp. 4037-4042, 2019b.
- Matino, I.; Dettori, S.; Colla, V.; Weber, V.; Salame, S. Forecasting blast furnace gas production and demand through echo state neural network-based models: Pave the way to off-gas optimized management, *Applied Energy*, v.253, pp. 113578, 2019c.
- Mhaya, A. M.; Huseien, G. F.; Faridmehr, I.; Abidin, A. R.; Alyousef, R.; Ismail, M. Evaluating mechanical properties and impact resistance of modified concrete containing ground Blast Furnace slag and discarded rubber tire crumbs. *Construction and Building Materials*, v. 295, pp. 123603, 2021.
- Muchnik, D. A.; Trikilo, A. I.; Lyalyuk, V. P.; Kassim, D. A. Coke Quality and Blast-Furnace Performance. *Coke and Chemistry*, v.61, pp. 12-18, 2018.
- Muraveva, I. G.; Togobitskaya, D. N.; Ivancha, N. G.; Bel'kova, A. I.; Nesterov, A. S. Concept Development of an Expert System for Selecting the Optimal Composition of a Multicomponent Blast-Furnace Charge and Functional and Algorithmic Structure. *Steel in Translation*, v.51, pp. 33-38, 2021.
- North, L.; Blackmore, K.; Nesbitt, K.; Mahoney, M. R. Methods of coke quality prediction: A review. *Fuel*, v.219, pp. 426-445, 2018.
- Oliveira, A. G.; Totola, L. B.; Bicalho, K. V.; Hisatugu, W. H. Prediction of compression index of soft soils from the Brazilian coast using artificial neural networks and empirical correlations. *Soils and Rocks*, v.43, pp. 109-121, 2020.
- Pandey, T. N.; Jagadev, A. K.; Dehuri, S.; Cho, S. B. A novel committee machine and reviews of neural network and statistical models for currency exchange rate prediction: An experimental analysis. *Journal of King Saud University - Computer and Information Sciences*, v.32, n.9, pp. 987-999, 2020.
- Pavlov, A. V.; Polinov, A. A.; Spirin, N. A.; Onorin, O. P.; Lavrov, V. V.; Gurin, I. A. Decision-Making Support in Blast-Furnace Operation. *Steel in Translation*, v.49, n.3, pp. 185-193, 2019.

- Quesada, D.; Valverde, G.; Larrañaga, P.; Bielza, C. Long-term forecasting of multivariate time series in industrial furnaces with dynamic Gaussian Bayesian networks, *Engineering Applications of Artificial Intelligence*, v.103, pp. 104301, 2021.
- Radhakrishnan, V. R.; Mohamed, A. R. Neural networks for the identification and control of blast furnace hot metal quality. *Journal of Process Control*, v.10, n.6, pp. 509-524, 2000.
- Rasul, M. G.; Tanty, B. S.; Mohanty, B. Modelling and Analysis of Blast Furnace Performance for Efficient Utilization of Energy. *Applied Thermal Engineering*, v.27, n.01, pp. 78-88, 2007.
- Reynolds, Q. G.; Rhamdhani, M. A. Computational Modeling in Pyrometallurgy: Part I. *JOM*, v.73, n.9, pp. 2658-2659, 2021.
- Rhamdhani, M. A.; Reynolds, Q. G. Computational Modeling in Pyrometallurgy: Part II. *JOM*, v.73, n.9, pp. 2885-2887, 2021.
- Saxén, H.; Pettersson, F. Nonlinear Prediction of the Hot Metal Silicon Content in the Blast Furnace. *ISIJ International*, 47, n.12, pp. 1732-1737, 2007.
- Semenov, Y. S.; Gorupakha, V. V.; Kuznetsov, A. M.; Semion, I. Y.; Schumel'chik, E. I.; Vashchenko, S. V.; Khudyakov, A. Y. Experience of Using Manganese-Containing Materials in Blast-Furnace Charge. *Metallurgist*, v.63, n.9, pp. 1013-1023, 2020.
- Sohn, S. K. I. Application of complex systems topologies in artificial neural networks optimization: An overview, *Expert Systems with Applications*, v.180, pp. 115073, 2021.
- Souza, P. V. C. Fuzzy neural networks and neuro-fuzzy networks: A review the main techniques and applications used in the literature, *Applied Soft Computing*, v.92, pp. 106275, 2020.
- Stein, S.; Leng, C.; Thornton, S.; Michel, R. A guided analytics tool for feature selection in steel manufacturing with an application to blast furnace top gas efficiency. *Computational Materials Science*, v.186, pp. 110053, 2021.
- Tan, M.; Bai, Y.; Zhang, H.; Li, G.; Wei, X.; Wang, A. Fluid typing in tight sandstone from wireline logs using classification committee machine. *Fuel*, v.271, pp. 117601, 2020.
- Tao, J.; Yu, Z.; Zhang, R.; Gao, F. RBF neural network modeling approach using PCA based LM-GA optimization for coke furnace system, *Applied Soft Computing*, v.111, pp. 107691, 2021.
- Völker, C.; Firdous, R.; Stephan, D.; Kruschwitz, S. Sequential learning to accelerate discovery of alkali-activated binders. *Journal of Materials Science*, v.56, n.28, pp. 15859-15881, 2021.
- Wang, Y. H.; Zhang, H.; Jiang, Z. G.; Zhao, G. Research of Coke Rate Prediction of Blast Furnace Based on Operative Characteristics of Auxiliary Resources. *Advanced Materials Research*, v.605-607, pp. 1792-1797, 2012.
- Wong, P. K.; Zhong, J.; Yang, Z.; Vong, C. M. Sparse Bayesian extreme learning committee machine for engine simultaneous fault diagnosis. *Neurocomputing*, v.174, Part A, pp. 331-343, 2016.
- Xu, Z. J.; Zheng, Z.; Gao, X. Q. Operation optimization of the steel manufacturing process: A brief review. *International Journal of Minerals, Metallurgy and Materials*, v. 28, n.8, pp. 1274-1287, 2021.
- Yi, Z.; Liu, Q.; Shao, H. Effect of MgO on Highly Basic Sinters with High Al₂O₃. *Mining, Metallurgy & Exploration*, v.38, n.5, pp. 2175-2183, 2021.
- Zablotskii, P. A.; Petrenko, V. A.; Kovshov, V. N. Procedure for Numerical Optimization of Blast-Furnace Charging Parameters Using a Mathematical Three-Factor Model. *Metallurgist*, v.61, n.3, pp. 175-178, 2017.
- Zhai, X.; Chen, M.; Lu, W. Fuel Ratio Optimization of Blast Furnace Based on Data Mining. *ISIJ International*, v.60, n.11, pp. 2471-2476, 2020.
- Zhang, J.; Li, S.; Li, Z. Investigation the synergistic effects in quaternary binder containing red mud, blast furnace slag, steel slag and flue gas desulfurization gypsum based on artificial neural networks. *Journal of Cleaner Production*, v.273, pp. 122972, 2020.
- Zhang, L.; Xue, Y.; Xie, Q.; Ren, Z. Analysis and neural network prediction of combustion stability for industrial gases. *Fuel*, v.287, pp.119507.
- Zhang, X.; Kano, M.; Matsuzaki, S. A comparative study of deep and shallow predictive techniques for hot metal temperature prediction in blast furnace ironmaking. *Computers & Chemical Engineering*, v.130, pp.106575, 2019b.
- Zhang, X.; Kano, M.; Matsuzaki, S. Ensemble pattern trees for predicting hot metal temperature in blast furnace. *Computers & Chemical Engineering*, v. 121, pp. 442-449, 2019a.
- Zhao, X.; Fang, Y.; Liu, L.; Xu, M.; Zhang, P. Ameliorated moth-flame algorithm and its application for modeling of silicon content in liquid iron of blast furnace based fast learning network. *Applied Soft Computing Journal*, v. 94, 106418, 2020.